

## Size-Dependent Behavior of Macromolecular Solids III: The Role of Entanglements

W. Wei and David CC LAM<sup>1</sup>

**Abstract:** Chain rotations in macromolecular solids are constrained by entanglements. The effects of constraints on strain deformation and strain gradient deformation were investigated using molecular dynamic (MD) simulation in this paper. The effects on the chains were examined by embedding the chains inside bent beams. For thick beams, the simulated elastic moduli for styrene butyl rubber (SBR), polyimide (PI) and polyethylene (PE) were in good agreement with elastic moduli reported in the literature. The elastic moduli varied linearly with entanglements and inversely with the molecular weight. For thin beams where strain gradients were non-negligible, the results showed that  $l_2$ , the higher order rotational length scale material parameter, also varied linearly with entanglements and inversely with the molecular weight. The linear dependence of  $E_0$  and  $l_2$  on entanglements can be correlated within specific chemistry such that the size dependent behavior of solids with the same monomer, but different molecular weight and entanglement can be predicted from the correlations. However, the correlations are chemistry specific, and the size-dependent behavior for a macromolecular solid cannot be casually predicted from the size-dependent behavior of another solid.

### 1 Single chain size dependence

Deformation of macro-molecular solids is determined by the rotational behavior of the molecular chains [Doi (1996); Treloar (2005)]. In the previous papers of this series [Lam, Keung and Tong (2010); Wei and Lam (2010)], the chain rotational behaviors as a function of deformation were investigated. The relations between rotation gradients and  $l_2$ , the higher order rotational material length scale parameter [Mindlin (1968); Ashby (1970); Fleck, Muller, Ashby and Hutchinson (1994)], were examined using single chain molecular simulations. The results showed that the molecular response to the elastic rotation gradients was rooted in the same mechanism as the molecular response to elastic strains. Based on the results, the

---

<sup>1</sup> Department of Mechanical Engineering, The Hong Kong University of Science and Technology, Clear Water Bay, Kowloon, Hong Kong SAR China. Email:david.lam@ust.hk

molecular basis for the higher order rotational length scale parameters was established.

In macromolecular solids, chain motions are constrained by neighboring chains and entanglements [Flory and Rehner (1943)]. Constrained movement requires additional energy, and solids with higher constraints would have higher  $E_0$  and  $l_2$ . Chain entanglements and interactions between chains were ignored in the previous paper [Wei and Lam (2010)]. The effects of these two constraints on  $E_0$  and  $l_2$  are investigated in this study. The constrained chain behaviors are modeled using a volume-bounded molecular dynamic model for materials with low elastic modulus (SBR) [Boháč and Vretenár (2004)], medium elastic modulus (PE) [Bartczak, Argon, Cohen and Weinberg (1999)] and high elastic modulus (PI) [Lee, Kim and Kwon (2010)]. The effects of the molecular weight and the entanglements have on  $E_0$  and  $l_2$  are investigated using the model.

## 2 Simulation methodology

In this study, a four-chain model was used to simulate the effects of chain interactions and entanglements (Fig. 2). The model was built using the molecular dynamic module (Forcite with Universal forcefield) in Materials Studio 5.0 from Accelrys [Maranganti and Sharma (2007); Zhu, Xiao, Feng, Ji, Ma and Xiao (2007)]. In the model, chains are anchored at the corners to simulate the constraints experienced by the chains in a solid, while the configurations of the segments between the anchors are allowed to vary dynamically within the box.  $M_c$  is the average molecular weight of the chains, and the volume of the cube is calculated from,

$$V = \frac{4M_c}{\rho \cdot N_A}, \quad (1)$$

where  $\rho$  is the density of the solid and  $N_A$  is the Avogadro number. To examine the deformation of the chains under different deformation, the cubic volume is placed on top of the neutral plane of the beam where the molecular cube is deformed according to the displacement field of the beam under pure bending [Norton (2006)]. After bending, the total deformation energy density of the four chains,  $u$  is determined via,

$$u = \frac{\Delta U}{V}, \quad (2)$$

where  $\Delta U$  is the integral of the deformation energy of the volume from the simulation. From conventional strain-based elasticity [Timoshenko and Goodier (1987)], the energy density of the volume in a bent beam is,

$$u = \frac{1 + 2\nu^2}{2} E_{eff} \kappa^2 V^{\frac{2}{3}}, \quad (3)$$

where  $\kappa$  is the beam curvature. When the beams are thick and the rotation gradients are negligible,  $E_{eff}$  is equal to the conventional elastic modulus  $E_0$ . When the beams are thin, additional rotations generated by the rotation gradients increases the  $E_{eff}$  beyond  $E_0$  [Fleck and Hutchinson (1997); Fleck and Hutchinson (2001)]. Accounting for contributions from  $l_2$ ,  $E_{eff}$  is given as [Lam, Yang, Chong, Wang and Tong (2003)],

$$E_{eff} = E_0 \left[ 1 + 3(1 - \nu) \frac{l_2^2}{h^2} \right] \quad (4)$$

where  $h$  is the beam thickness and  $\nu$  is the Poisson's ratio of the solid. In this investigation, the effects of entanglements on  $E_0$  and  $l_2$  were investigated using bent beams with different beam thicknesses using molecular dynamics.

In molecular dynamic simulation, the energy of a single isolated chain (Fig. 1) is dependent on strain, but is also a function its configuration which varies dynamically with time. The energy variation of a chain over time is shown in Fig. 1, and the cumulative energy distribution is shown in the insert. In this investigation, the energy of the chains in the simulated volume during beam bending was modeled using molecular dynamics. The deformation energy density  $u$  was calculated from the peak energies of stable energy distributions.

In the simulation, chains anchored at the corners without entanglement (Fig. 2a) were used as the reference state for comparison and benchmarking with experimental data from the literature. After benchmarking, the number of entanglements (Fig. 2b) in the volume, was increased from 0 to 6 to investigate the effects of entanglements on  $E_0$  and  $l_2$ .

### 3 Results

#### 3.1 Elastic modulus

The effect of the molecular weight and entanglements on  $E_0$  and  $l_2$  of soft styrene butyl rubber (SBR), medium polyethylene (PE), and stiffen polyimide (PI) were simulated. The simulation setting used is shown in Tab. 1.

Table 1: Parameters used in simulation setting

		PE	SBR	PI
Figure 3	Beam thickness $h$ ( $\mu\text{m}$ )	200	100	100
	Simulated $M_c$ (g/mol)	112	428	3220
Figure 7 & Figure 8	Beam thickness $h$ ( $\mu\text{m}$ )	200-100	100-1	100-1
	Simulated $M_c$ (g/mol)	1960	1712	3220

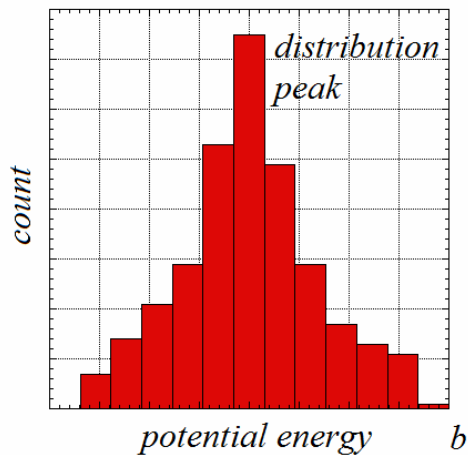
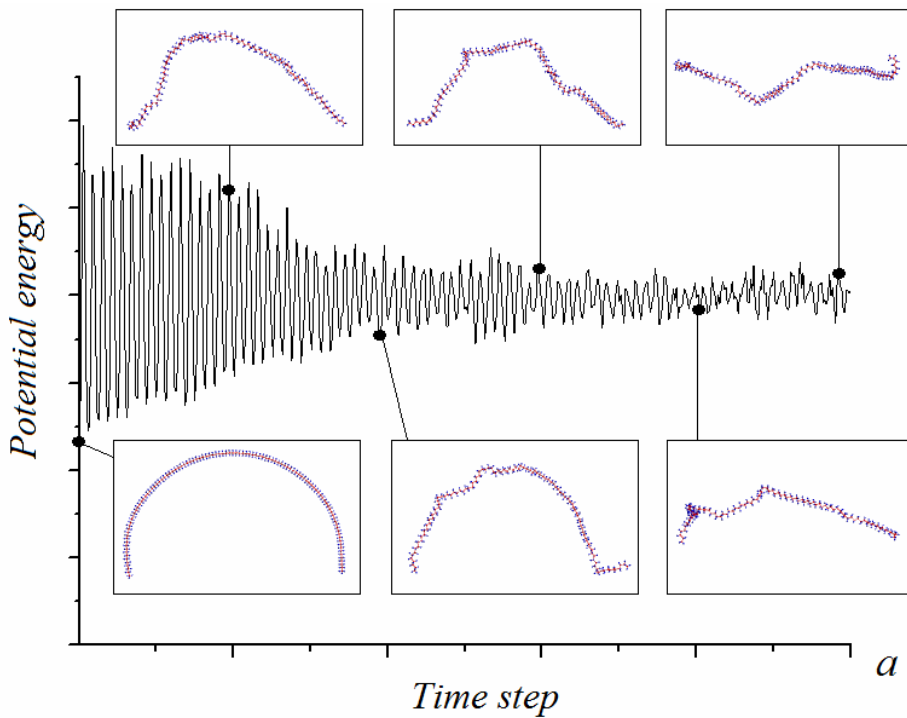


Figure 1: a) A single isolated chain; b) variation of the energy of a single chain as its configuration dynamically varies as a function of time and c) its cumulative distribution.

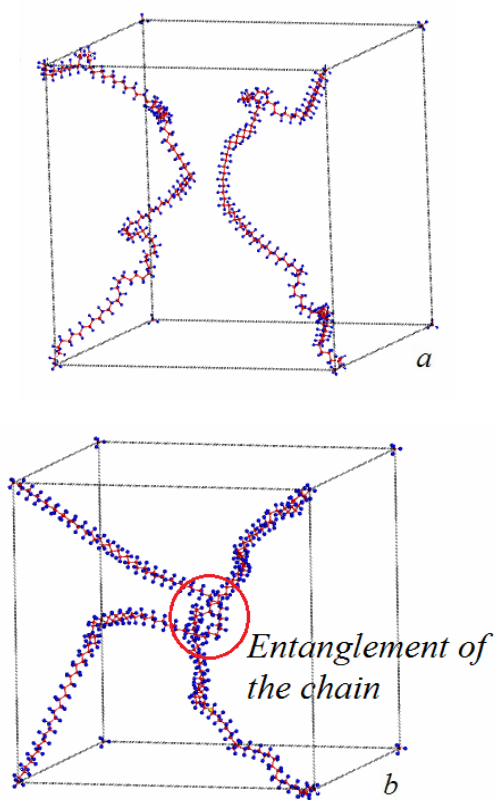


Figure 2: a) Two separate, but interacting chains; and b) two entangled chains.

A comparison of the elastic modulus from the simulation and from the literature is shown in Fig. 3. The comparison showed that the elastic moduli from simulations for all three solids are within 10% of the experimental value (Tab. 2). This indicated that the boundary conditions for the 4-chain model were set properly to account for the external constraints.

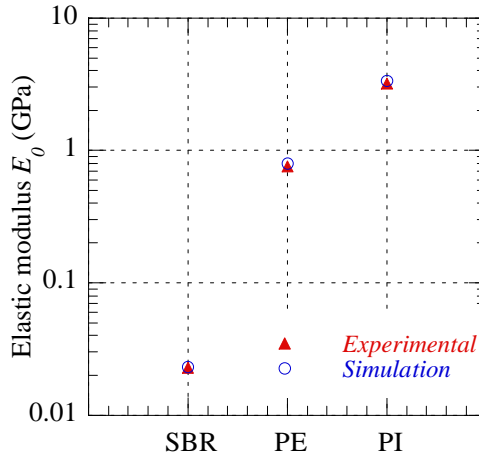


Figure 3: Comparison of the elastic modulus from simulation with experimental elastic modulus for PE, SBR and PI.

Table 2: Comparison of material properties

	SBR	PE	PI
Density $\rho$ (g/cm <sup>3</sup> )	1.043	0.9565	1.43
Experimental $E_0$ (GPa)	0.023	0.756	3.2
Molecular weight $M_c$ <sup>1</sup> (g/mol)	335.92	93.724	3200.0
Entanglement density $\nu_{e,0}$ <sup>2</sup> (mol/m <sup>3</sup> )	3.105E-06	1.021E-04	4.469E-04
Simulation $E_0$ (GPa)	0.0231	0.798	3.35

### 3.2 Effect of molecular weight

Using the benchmarked procedure, the effective elastic moduli ( $E_{eff}$ ) of solids with different molecular weights were simulated and plotted in Fig. 4. For clarity, the size of the chain is described by the number of monomers in the chain as,

$$N = \frac{M_c}{m_0} \tag{5}$$

where  $M_c$  is the molecular weight of one chain and  $m_0$  is the molecular weight of one monomer. The results showed that solids with lower molecular weight, i.e., shorter chains, have stronger size effect. From  $E_{eff}$ , the materials properties,  $E_0$  and  $l_2$ , can be delineated using Eq. (4). The effects of molecular weight on  $E_0$  for PE, SBR and PI are shown in Fig. 5. The figure showed that the  $E_0$  is inversely dependent on the number of monomers, and by definition (Eq. (5)), is also inversely dependent on the molecular weight. The results are in agreement with the classical dependence as predicted by rubber elasticity [Abu-Abdeen (2001); Treloar (2005); Abu-Abdeen and Elamer (2010)] is reproduced successfully by the model. The variation of  $l_2$  with the molecular weight is shown in Fig. 6. For all three families of solids,  $l_2$  also varied linearly with the inverse of molecular weight.

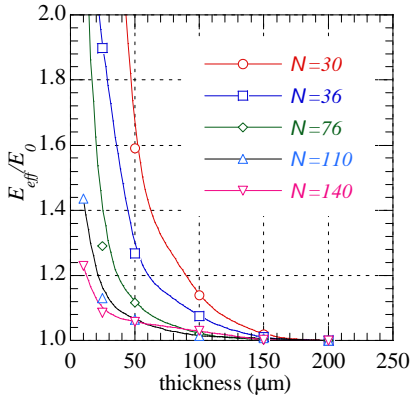


Figure 4: Effective elastic modulus of PE as a function of the beam thickness, where  $E_0$  is the conventional size-independent elastic modulus of PE. The curves are generated by fitting Eq.(4) to the data.

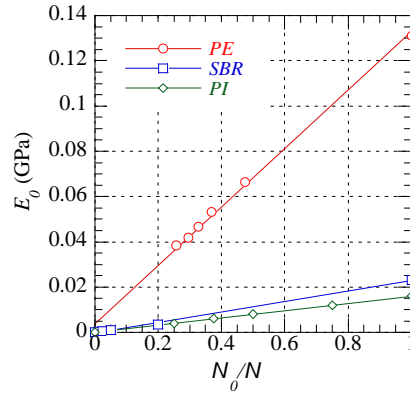


Figure 5: The influence of the number of monomers on  $E_0$ .  $1/N$  on the X-axis is normalized by its maximum value  $1/N_0$ , which are 0.028, 1, 0.5 for PE, SBR and PI, respectively.

### 3.3 Effect of entanglements

In macromolecular solids, the chains are constrained from movement by the entanglements and the neighboring chains. In the simulation, the baseline constraints were simulated by the corner anchors. The resulting elastic moduli were in good agreement with experimental elastic moduli (Fig. 3). The chains within the box were unentangled and their movement was constrained only by the wall and their neighbors in the baseline model. By threading the chains, up to 6 entanglements

can be simulated in our model. The effects of entanglements  $v_e$  on  $E_0$  and  $l_2$  are plotted in Fig. 7 and Fig. 8. The results showed that  $E_0$  and  $l_2$  increased linearly with  $v_e$ .

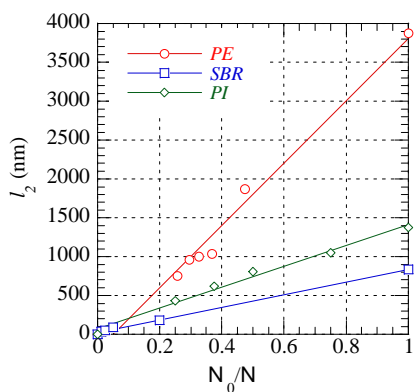


Figure 6: The influence of number of monomers on  $l_2$ .  $1/N$  on the X-axis is normalized by its maximum value  $1/N_0$ , which are 0.028, 1, 0.5 for PE, SBR and PI, respectively.

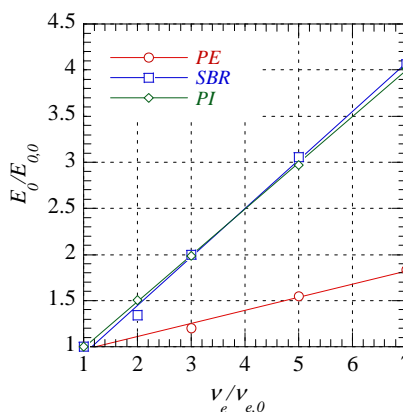


Figure 7: The influence of  $N_{ent}$  on  $E_0$  for PE, SBR and PI. The elastic modulus on the y-axis is normalized by  $E_0$  of solids without entanglements, i.e.,  $E_{0,0}(PE) = 3.85E - 2$  GPa,  $E_{0,0}(SBR) = 4.51E - 3$  GPa and  $E_{0,0}(PI) = 3.35$  GPa.

#### 4 Discussion

The simulation results showed that the molecular weight and entanglements have analogous effects on the elastic modulus  $E_0$  and  $l_2$ . Lowering the molecular weight reduces the distance between the anchors and increases the constraint on the chains. Since the deformation mechanism underpinning  $E_0$  is chain rotation, stronger constraints would increase  $E_0$ . Analogously,  $l_2$  is also inversely dependent on the molecular weight since both  $l_2$  and  $E_0$  are material properties underpinned by chain rotation of the same molecules.

Similar to the inverse dependence on the molecular weight, adding entanglements into the solid volume increases the constraint on chain movement and increases  $l_2$  and  $E_0$ . In fact,  $E_0$  and  $l_2$  for solids with the same chemistry system can be correlated linearly.  $E_0$  and  $l_2$  can be predicted for solids with different entanglements and molecular weight can be predicted from the correlations, i.e., from known molecu-



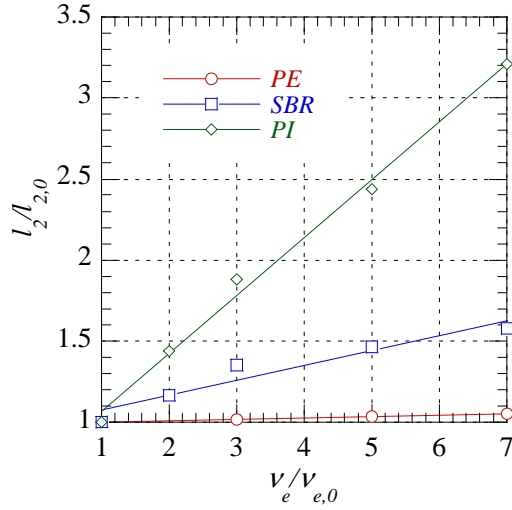


Figure 8: The influence of  $N_{ent}$  of  $l_2$  from PE, SBR and PI simulation. The  $l_2$  on the y-axis is normalized by  $l_2$  of solids without entanglements, i.e.,  $l_{2,0}(PE) = 747.75$  nm,  $l_{2,0}(SBR) = 194.88$  nm and  $l_{2,0}(PI) = 429.14$  nm.

lar weight and entanglement series of  $E_0$  and  $l_2$ . However, the correlations are not generalizable across different chemistries; and further work is needed to investigate the effect of chemistry has on  $E_0$  and  $l_2$ .

## 5 Conclusions

Simulations were conducted to examine the effects of molecular weight and entanglement on the size dependence of macromolecular solids. The simulations were benchmarked using solids that are soft (SBR), medium (PE) and stiff (PI). The comparisons showed that the inverse dependence of simulated elastic modulus  $E_0$  on the molecular weight is in good agreement with literature. The simulation also showed that  $l_2$  varied linearly with entanglements and inversely with the molecular weight. Both dependences can be correlated with  $E_0$ 's dependence on entanglement and molecular weight, but the correlations are limited to solids that share the same macromolecular chemistry, and are not generalizable to other solids with different chemistry.

## References

- Abu-Abdeen, M.** (2001): Degradation of the mechanical properties of composite vulcanizates loaded with paraffin wax. *Journal of Applied Polymer Science*, vol. 81, pp. 2265-2270
- Abu-Abdeen, M.; Elamer, I.** (2010): Mechanical and swelling properties of thermoplastic elastomer blends. *Materials & Design*, vol. 31, pp. 808-815
- Ashby, M. F.** (1970): The Deformation of Plastically Non-homogeneous Materials. *Philosophical Magazine* vol. 21, pp. 399-424
- Bartczak, Z.; Argon, A. S.; Cohen, R. E.; Weinberg, M.** (1999): Toughness mechanism in semi-crystalline polymer blends: II. High-density polyethylene toughened with calcium carbonate filler particles. *Polymer*, vol. 40, pp. 2347-2365
- Bohac, V.; Vretenar, V.** (2004): Thermophysical Properties of Styrene Butadiene Rubber Filled With Pine Tree Particles Measured by the Transient Plane Source Technique.
- Doi, M.** (1996): Introduction to polymer physics. *Clarendon Press*
- Fleck, N. A.; Muller, G. M.; Ashby, M. F.; Hutchinson, J. W.** (1994): Strain gradient plasticity - Theory and experiment. *Acta Metallurgica Et Materialia*, vol. 42, pp. 475-487
- Fleck, N. A.; Hutchinson, J. W.** (1997): Strain gradient plasticity. *Adv. in Appl. Mech.*, vol. 33, pp. 295-361
- Fleck, N. A.; Hutchinson, J. W.** (2001): A reformulation of strain gradient plasticity. *Journal of the Mechanics and Physics of Solids*, vol. 49, pp. 2245-2271
- Flory, P. J.; Rehner, J.** (1943): Statistical theory of chain configuration and physical properties of high polymers. *Annals of the New York Academy of Sciences*, vol. 44, pp. 419-429
- Lam, D. C. C.; Yang, F.; Chong, A. C. M.; Wang, J.; Tong, P.** (2003): Experiments and theory in strain gradient elasticity. *Journal of the Mechanics and Physics of Solids*, vol. 51, pp. 1477-1508
- Lam, D. C. C.; Keung, L. H.; Tong, P.** (2010): Size-Dependent Behavior of Macromolecular solids II: Higher-Order Viscoelastic Theory and Experiments. *CMES: Computer Modeling in Engineering & Sciences*, vol. 66, pp. 73-99
- Lee, G.; Kim, Y.; Kwon, D.** (2010): Mechanical characterization of polymer passivation layer in semiconductor applications using IIT and FEA. *Microelectronic Engineering*, vol. 87, pp. 2288-2293
- Maranganti, R.; Sharma, P.** (2007): A novel atomistic approach to determine strain-gradient elasticity constants: Tabulation and comparison for various metals,

semiconductors, silica, polymers and the (Ir) relevance for nanotechnologies. *Journal of the Mechanics and Physics of Solids*, vol. 55, pp. 1823-1852

**MINDLIN, N. N. E. a. R. D.** (1968): On first strain gradient theories in linear elasticity. *International Journal of Solids and Structures*, vol. 4

**Norton, R. L.** (2006): *Machine design :an integrated approach*. 3<sup>rd</sup> ed. Upper Saddle River, NJ: Prentice Hall.

**Timoshenko, S.; Goodier, J. N.** (1987): *Theory of elasticity*. 3<sup>rd</sup> ed. New York: McGraw-Hill.

**Treloar, L. R. G.** (2005): *The physics of rubber elasticity*. 3<sup>rd</sup> ed. Oxford: Clarendon Press.

**Wei, W.; Lam, D. C. C.** (2010): Size-Dependent Behavior of Macromolecular Solids I: Molecular Origin of the Size Effect. *Computer Modeling in Engineering & Sciences*, vol. 64, pp. 213-226

**Zhu, W.; Xiao, J. J.; Feng, Z.; Ji, G. F.; Ma, X. F.; Xiao, H. M.** (2007): Molecular dynamics simulation of elastic properties of HMX/TATB composite. *Acta Chimica Sinica*, vol. 65, pp. 1223-1228

